Gas Transfer at Water Surfaces 2010, edited by S. Komori, W. McGillis, R. Kurose,
Kyoto University Press, 2011, ISBN 978-4-87698-560-9, pp. 358-367
doi: 10.5281/zenodo.14956

The 2009 SOPRAN active thermography pilot experiment in the Baltic Sea

Uwe Schimpf[1], Leila Nagel[1], and Bernd Jähne[1,2]

[1] *Institute of Environmental Physics, University of Heidelberg, Im Neuenheimer Feld 229, 69120 Heidelberg, Germany, E-mail: {Uwe.Schimpf,Leila.Nagel}@iup.uni-heidelberg.de*

[2] *Heidelberg Collaboratory for Image Processing (HCI) at the Interdisciplinary Center for Scientific Computing, University of Heidelberg, Speyerer Str. 6, 69115 Heidelberg, Germany, E-mail: Bernd.Jaehne@iwr.uni-heidelberg.de*

Abstract.

Heat is used as a proxy tracer for gases to investigate the transport across the sea-surface microlayer. A further development of the active controlled flux technique (ACFT) is presented. A periodically varying heat flux density is forced onto a rectangle area at the water surface by a CO_2 laser. The resulting variation in sea surface temperature is imaged with a calibrated IR-camera. The time constant of the transfer process is estimated by the amplitude damping of the temperature response in the Fourier domain. A pilot experiment in the Baltic Sea was conducted and heat transfer rates were determined. Applying Schmidt number scaling, the measured transfer rates are in good agreement with empirical gas transfer wind speed relationships for moderate wind speeds (4-6 ms^{-1}). At high wind speed (12 ms^{-1}), the ACFT transfer rates are lower, which might be explained by the fact that heat transport is insensitive to bubble-mediated gas transfer.

Key Words: active controlled flux technique, heat transfer velocity, Schmidt

number scaling, periodic heat flux forcing, small scale air-sea interaction

1. Introduction

The air-water phase boundary constitutes the bottleneck for the transfer of gases into the ocean. For slightly soluble and inert gases this transfer is controlled by the aqueous mass boundary layer, where the molecular diffusion limits the gas transfer rate. Knowledge about the parameters that influence the transfer across the aqueous boundary layer increased considerably in recent years, e.g. (Wanninkhof et al., 2009), but the physical processes controlling the mass boundary layer are not yet fully understood. Conventionally, the gas transfer velocity is measured by direct flux methods (e.g. eddy covariance/accumulation techniques, atmospheric concentration profile methods), or mass balance methods. The transfer velocity, k_g, is defined by the ratio of the gas flux density j across the air-sea interface and the concentration difference Δc between the surface and the well-mixed bulk:

$$k_g = \frac{j}{\Delta c}. \tag{1}$$

The physical concept that a gradient drives a flux, with the flux density proportional to the diffusion coefficient and the concentration gradient, applies to the transport of heat, momentum, and mass (Jähne and Haußecker, 1998).Consequently, equation (1) can be rewritten for the transport of heat across the air-sea interface as:

$$k_h = \frac{q_{net}}{\rho\, C_p\, \Delta T}, \tag{2}$$

where ΔT is the skin-bulk temperature difference, q_{net} the net air-sea heat flux density at the water surface in absence of downwelling solar radiation, ρ the density of water and C_p the specific heat capacity of water. In order to compare the transfer velocities of scalar tracers (e.g. heat and gas), knowledge of the dimensionless Schmidt number $Sc = \nu/D$, where ν is the kinematic viscosity of water and D the diffusion coefficient, of the observed species is required. Applying Schmidt number scaling, the heat transfer velocity is extrapolated to a gas transfer velocity according to Jähne et al. (1987):

$$k_g = k_h \left(\frac{Sc}{Pr}\right)^{-n}, \tag{3}$$

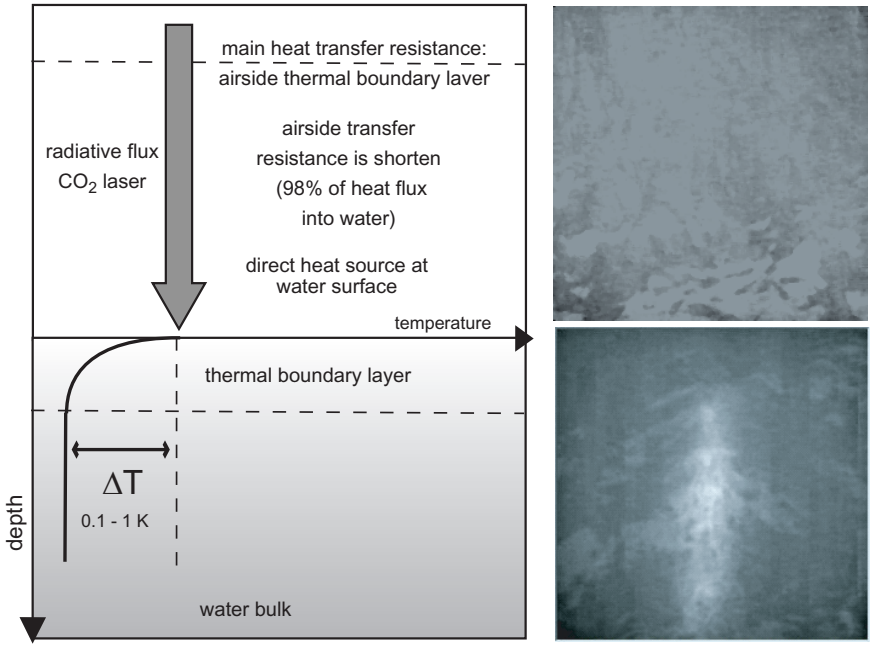

Figure 1. Active controlled flux technique: a heat flux density is forced directly onto the water surface by a CO_2 laser resulting in a temperature gradient across the thermal sublayer in the order of $0.1 - 0.5\,\mathrm{K}$. Infrared image of water surface before (top) and while (bottom) heating up the water surface.

with the Prandtl number Pr of heat in water and the Schmidt number exponent n (2/3 for a smooth surface, 1/2 for a wavy surface). The Prandtl number is defined as $Pr = \nu/D_h$, where $D_h = \lambda/\rho C_p$ is the thermal diffusivity and λ the thermal conductivity.

This scaling might cast some doubts (Asher et al., 2004) on the validity of the extrapolation from heat to gas fluxes, because the diffusive sublayer is around ten times thinner than the thermal sublayer due to the large difference of the Prandtl ($Pr = 7$) and the Schmidt number (e.g. $Sc = 660$ for CO_2 in sea water at $T = 20°\mathrm{C}$).

Direct flux techniques or mass balance methods use either a naturally occurring concentration difference or force a concentration difference by purposeful injecting a tracer and measure the resulting flux density to infer the transfer velocity.

The active controlled flux technique simply inverts this procedure: a controlled heat flux density forces a skin-bulk temperature difference across the thermal sublayer (see figure 1). The characteristic time scale, $t_\star$, of the transfer process is measured and the heat transfer rate, k_h, calculated according to:

$$k_h = \sqrt{\frac{D_h}{t_\star}}, \tag{4}$$

where D_h is the diffusivity of heat in water. In the first realization of the active controlled flux method, Jähne et al. (1989) forced a periodic heat flux density onto the water surface using chopped infrared radiation. The temperature response of the heated area at the water surface was detected with a point measuring radiometer. Later, Haußecker et al. (1995) used an IR-camera to track a small patch at the water surface heated up by a short pulse of a CO_2 laser. The temporal temperature decay of the patch is fitted based on solving the diffusive transport equation including the surface renewal model (Higbie, 1935; Danckwerts, 1951) as a first-order process. The time constant of the decay is identified with the surface renewal time scale and the heat transfer rate is calculated. A further method for the analysis of the decay curves was proposed by Atmane et al. (2004), whereas the diffusive transport is combined with a Monte Carlo simulation of the renewal process based on the surface penetration model (Harriott, 1962). Zappa et al. (2004) and Asher et al. (2004) measured a scaling factor of roughly 2.5 between the gas and heat transfer velocity when they applied the active controlled flux technique.

Following Asher et al. (2004) the surface penetration theory provides a more accurate conceptual model for air-sea gas exchange which is supported by the work of Jessup et al. (2009) who found evidence for complete and partial surface renewal at an air-water interface. The advantage deriving heat transfer rates by the decay method is the independence of the applied heat flux density but the major drawback is the model dependence. Furthermore, lateral expansion of the heated patch (diffusion and turbulent transport) might increase the decay rate and would pretend a shorter surface renewal time scale and therefore a higher transfer rate.

To overcome the above mentioned drawbacks, two modifications of the ACFT (areal heating and periodic heat flux forcing) were realized. The details and the two available techniques (temporal decay method and amplitude damping in the frequency domain) to derive the characteristic time scale of the transfer process are described in section 2. An overview of the new ACFT setup and the technical details during the first pilot experiment, which was conducted in

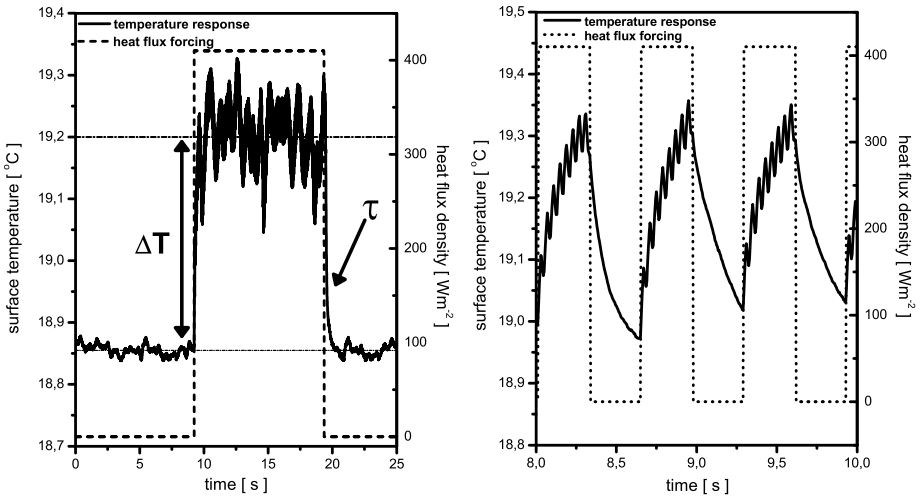

Figure 2. Periodic heat flux forcing and temperature response for low (0.488 Hz) and high forcing frequency (1.562 Hz), along-wind scan frequency 25 Hz both. Data taken in the Heidelberg Aeolotron at a wind speed of 5 m/s.

April, 2009 in the Baltic Sea, is given in section 3. The Schmidt number scaled gas transfer rates of both methods are in good agreement and the results are discussed in section 4. in conjunction with the commonly used environmental parameterizations of the transfer rate with wind speed.

2. Method

In the setup of the ACFT two modifications were done. Instead of a small patch a rectangle area at the water surface is heated up (see figure 1). Consequently more pixels are available for the analysis and lateral transport is, at least to some extent, taken into account. Additionally, periodic heat flux forcing was applied, as proposed by Jähne et al. (1989). The time constant of the transfer process is estimated by looking at how the thermal boundary layer responds to periodic forcing. The thermal boundary layer might be considered similar to a low pass filter. The input function is a periodic varying heat flux density $Q(t)$ and the output is the temperature response $T(t)$. The frequency response of the temperature $|\tilde{T}(\omega)|$ delivers the cut-off frequency, i.e. the time constant of the transfer process. It is important to note that in contrast to the decay

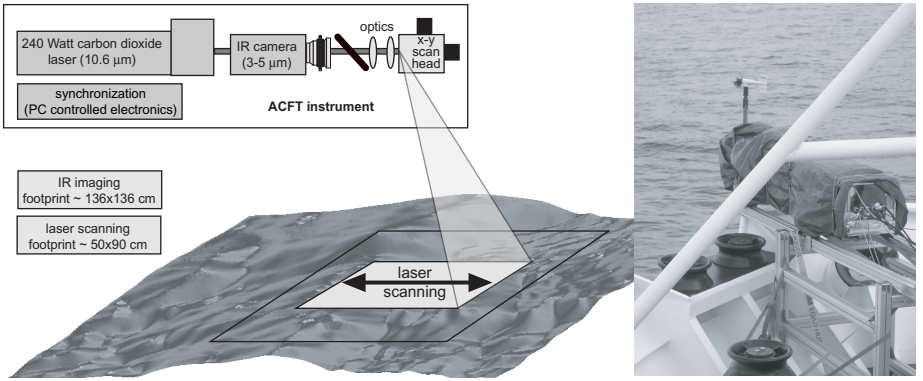

Figure 3. Schematic setup of the ACFT instrument and deployment during the research cruise AL-336 onboard FS Alkor in the Baltic Sea, April, 2009.

method this technique does not depend on any model assumptions and the net heat flux density has not to be known in order to estimate the characteristic time scale. For low frequencies ($\omega t_\star \ll 1$), i.e. the frequency with which the laser is switched on and off, the mean surface temperature remains constant at the equilibrium value for zero frequency (i.e. a constant flux) when the laser is switched on. As soon as the forcing stops, the temperature decays with the typical time constant (see figure 2). The temperature decay of the heated area is fitted based on surface renewal theory and the time constant is estimated (Haußecker, 1996). When the forcing frequency ω is increased, i.e. $\omega t_\star \gg 1$, the temperature response does not come into equilibrium, starts lagging behind the heat flux forcing and is decreasing (see figure 2) The larger the frequency, the shallower the heat will penetrate and is therefore restricted to molecular diffusion and thus the amplitude of the temperature signal is damped, whereas $|\tilde{T}(\omega)| \propto \omega^{-0.5}$ (Jähne et al., 1989). The analysis of the temperature response is done in the frequency domain. The damping is calculated by dividing the power spectra of the of the forcing signal $|\tilde{j}(\omega)|$ by the spectra of the temperature response $|\tilde{T}(\omega)|$. The intersection of the equilibrium and the diffusion range delivers the cut-off frequency and thus the time constant of the transfer process (see figure 4), independently of any model and without knowing the applied heat flux density.

3. Experiments

The active thermography pilot experiment was conducted within the framework of the SOPRAN (Surface Ocean Processes in the Anthropocene) initiative. The ACFT instrument was mounted at the bow of the research Vessel FS Alkor (see figure 3) during the research cruise AL-356 in the Baltic Sea which took place in April, 2009. During six deployments the wind speed ranged from $5.3\,\mathrm{ms}^{-1}$ to $12.5\,\mathrm{ms}^{-1}$. The digital IR-camera CMT 256HS (Thermosensorik, Erlangen) observes a footprint (size $\approx 136 \times 130\,\mathrm{cm}$) at the water surface at a frame rate of 400 Hz. The focal plane array detector (256×256 pixels) is sensitive in the wavelength regime from 3.1 to $5.3\,\mu\mathrm{m}$ with a NEΔT (noise equivalent temperature difference) of 18 mK and was calibrated using an areal blackbody source (2004G, Santa Barbara Infrared, Santa Barbara, CA). An area (size $\approx 90 \times 50\,\mathrm{cm}$) at the water surface was heated up by a 200 W continuous wave CO_2 laser (firestar f200, Synrad Inc., Edmonds, WA) emitting at a wavelength of $10.6\,\mu\mathrm{m}$. The laser beam is extended in cross wind direction by two focal lenses and in along wind direction with a mirror positioning system (Micro Max 671, Cambridge Technology Inc., Cambridge, MA) resulting in a heat flux density of $q \approx 413\,\mathrm{Wm}^{-2}$. The image acquisition, laser control, and scan unit was synchronized by a self-designed integrated circuit.

4. Results and discussion

By analyzing the temperature calibrated image sequences at low frequencies, for each deployment a heat transfer rate is determined by the decay method (see section 2.). Considering all frequencies during one deployment the temperature response in the frequency domain is calculated and the heat transfer rate estimated. The heat transfer rates are scaled to gas transfer rates applying Schmidt number scaling (equation (3)) using a Schmidt number exponent $n = 1/2$ (wavy surface) which seems appropriate for the wind speed range of $5.3\,\mathrm{ms}^{-1}$ to $12.5\,\mathrm{ms}^{-1}$. In figure 5 the Schmidt number scaled transfer velocities during the Baltic Sea pilot experiment in April, 2009 of both methods are plotted versus wind speed. The error bars indicate the standard deviation of 5 measurements and wind speed during sampling time. At moderate wind speeds (5 to $9\,\mathrm{ms}^{-1}$) the scaled transfer rates are in good agreement with empirical gas transfer wind speed relationship proposed by Nightingale et al. (2000). The two methods agree within the error bars and the data does not show a scaling factor between heat and gas exchange rate as measured by Zappa et al. (2004) and Asher et al. (2004) when they applied the active controlled flux technique. Due to the high solubility (dimensionless solubility $\alpha \approx 3900$ (Jähne, 1985))

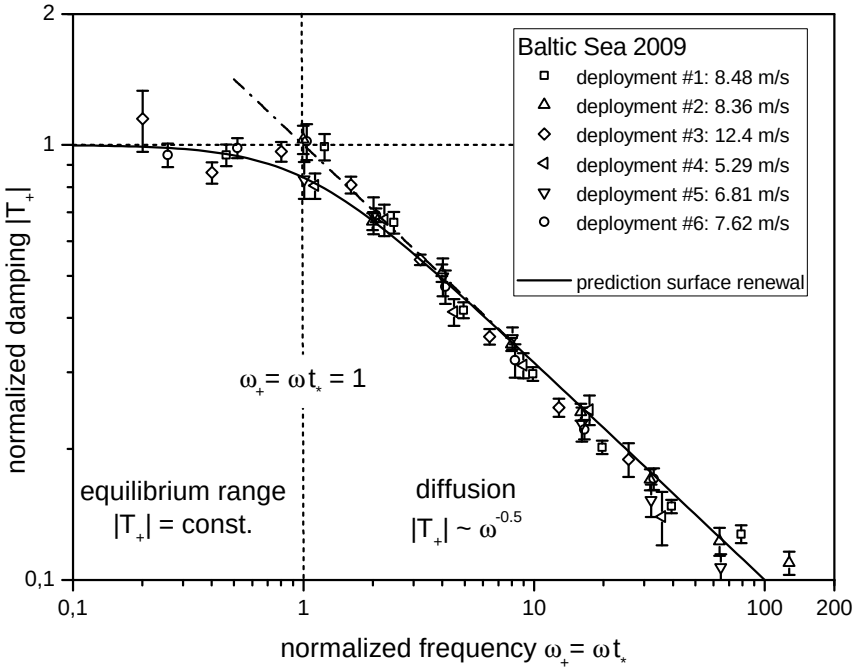

Figure 4. Normalized amplitude damping $|\tilde{T}_+(\omega)|$ versus normalized frequency $\omega_+ = \omega t_\star$ of the complete data set and theoretical prediction of the surface renewal model.

heat is actually an airside controlled tracer. Applying the ACFT the airside transfer resistance is short-circuited (about 98% of the laser induced heat flux density arrives at the surface and is absorbed within the top 20 micrometers) and therefore the radiative flux represents a direct heat source at the water surface. The ACFT is insensitive to bubble-mediated gas transfer since bubbles are not affected by the heating. Breaking waves not only create bubbles but also induce additional turbulence (Jähne, 1991) which in turn increases heat and gas exchange. The ACFT is sensitive to the increased turbulence, but not to the effect of the bubbles on gas transfer, i.e. the heat mimics the behavior of a tracer with high solubility and measures only a part of the transfer process directly at the water surface. This might explain why ACFT transfer rates are

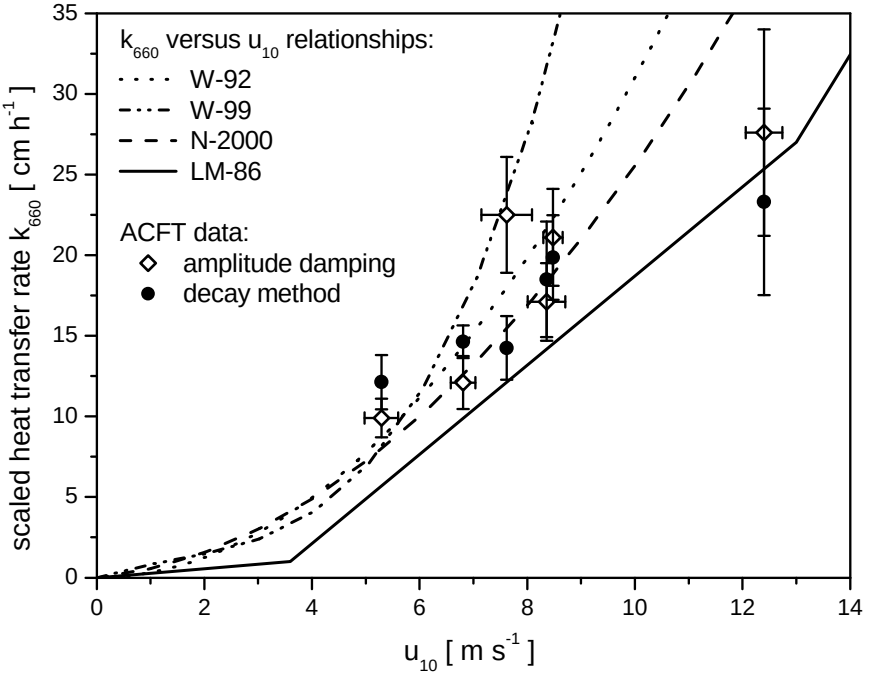

Figure 5. Schmidt number scaled transfer rates from the decay method and periodic forcing during the Baltic Sea pilot experiment in April, 2009. For comparison the empirical relationships of Liss and Merlivat (1986); Wanninkhof (1992); Wanninkhof and McGillis (1999); Nightingale et al. (2000) are shown.

lower at high wind speed ($12\,\mathrm{ms}^{-1}$) than the empirical gas transfer wind speed relationships. Thus, if the Schmidt number scaling between heat and gas is valid, coincident measurements of the transfer coefficient of gases might allow to distinguish and quantify the different mechanisms which contribute to air-water gas transfer.

The estimates of time constant by the amplitude damping have a fairly long sampling time (order of forty minutes) but are model independent. However, the decay method shows a high variability in the transfer rates due to the short sampling time (order of one minute) but depends on surface renewal theory. This variability of the transfer velocities when plotted versus wind speed clearly

indicates that not only the wind speed but also other processes such as the wave field and surfactants influence near-surface turbulence and thus air-water gas transfer (Frew et al., 2004).

5. Conclusions and outlook

The first field study with the modified ACFT delivered very promising results. Two different analysis methods were used to infer heat transfer rates by the active controlled flux technique, which gave - within the experimental errors and short-term variability - identical results. The decay method has a short sampling time (order of one minute) but depends on surface renewal theory. The analysis of the temperature response in the frequency domain has a fairly long sampling time (order of forty minutes) but does not depend on any model assumptions.

Ongoing laboratory studies with simultaneous measurements of heat and gas exchange are carried out in the Heidelberg Aeolotron, which focus on the Schmidt number dependence of the transfer process for a more precise scaling from heat to gas transfer rates. Within SOPRAN-II project (2010 until 2012) more cruises in the Baltic Sea, partly with coincident eddy correlation measurements are planned.

Acknowledgements

We would like to thank the crew of the FS Alkor for their assistance in conducting the measurements. We wish to thank B. Schneider and R. Schmidt of the Leibniz-Institut für Ostseeforschung and R. Rocholz and G. Balschbach of the Institut für Umweltphysik, for preparation and accomplishment of the field experiment. We gratefully acknowledge the support and funding by the BMBF Project SOPRAN (contract 03F0462F) - Surface Ocean Processes in the Anthropocene.

References

Asher, W. E., A. T. Jessup, and M. A. Atmane (2004), Oceanic application of the active controlled flux technique for measuring air-sea transfer velocities of heat and gases, *J. Geophys. Res.*, *109*, C08S12.

Atmane, M. A., W. Asher, and A. T. Jessup (2004), On the use of the active infrared technique to infer heat and gas transfer velocities at the air-water interface, *J. Geophys. Res.*, *109*, C08S14.

Danckwerts, P. V. (1951), Significance of a liquid-film coefficients in gas absorption, *Ind. Eng. Chem.*, *43*, 1460–1467.

Frew, N. M., E. J. Bock, U. Schimpf, T. Hara, H. Haußecker, J. B. Edson, W. R. McGillis, R. K. Nelson, B. M. McKeanna, B. M. Uz, and B. Jähne (2004), Air-sea gas transfer: Its dependence on wind stress, small-scale roughness, and surface films, *J. Geophys. Res.*, *109*, C08S17.

Harriott, P. (1962), A random eddy modification of the penetration theory, *Chem. Eng. Sci.*, *17*, 149–154.

Haußecker, H. (1996), *Messung und Simulation von kleinskaligen Austauschvorgängen an der Ozeanoberfläche mittels Thermographie*, Phd thesis, Faculty for Physics and Astronomy, Univ. Heidelberg.

Haußecker, H., S. Reinelt, and B. Jähne (1995), Heat as a proxy tracer for gas exchange measurements in the field: principles and technical realization, in B. Jähne and E. C. Monahan (Eds.), *Air–Water Gas Transfer: Selected Papers from the Third International Symposium on Air–Water Gas Transfer*, pp. 405–413, AEON Verlag & Studio Hanau, Heidelberg.

Higbie, R. (1935), The rate of absorption of a pure gas into a still liquid during short periods of exposure, *Trans. Am. Inst. Chem. Eng.*, *31*, 365–389.

Jessup, A. T., W. E. Asher, M. Atmane, K. Phadnis, C. J. Zappa, and M. R. Loewen (2009), Evidence for complete and partial surface renewal at an air-water interface, *Geophys. Res. Lett.*, *36*, 1–5.

Jähne, B. (1985), *On the transfer processes at a free air-water interface*, Habilitation thesis, Institute of Environmental Physics, Faculty for Physics and Astronomy, Univ. Heidelberg.

Jähne, B., K. O. Münnich, R. Bösinger, A. Dutzi, W. Huber, and P. Libner (1987), On the parameters influencing air-water gas exchange, *J. Geophys. Res.*, *92*, 1937–1950.

Jähne, B., P. Libner, R. Fischer, T. Billen, and E. J. Plate (1989), Investigating the transfer process across the free aqueous boundary layer by the controlled flux method, *Tellus*, *41B*(2), 177–195.

Jähne, B. (1991), New experimental results on the parameters influencing air-sea gas exchange, in S. C. Wilhelms and J. S. Gulliver (Eds.), *Air-Water Mass Transfer, selected papers from the 2nd International Symposium on Gas Transfer at Water Surfaces, September 11–14, 1990, Minneapolis, Minnesota*, pp. 582–592, ASCE.

Jähne, B. and H. Haußecker (1998), Air-water gas exchange, *Annu. Rev. Fluid Mech.*, *30*, 443–468.

Liss, P. S. and L. Merlivat (1986), Air-sea gas exchange rates: Introduction and synthesis, in P. Buat-Menard (Ed.), *The role of air-sea exchange in geochemical cycling*, pp. 113–129, Reidel, Boston, MA.

Nightingale, P. D., G. Malin, C. S. Law, A. J. Watson, P. S. Liss, M. I. Liddicoat, J. Boutin, and R. C. Upstill-Goddard (2000), In situ evaluation of air-sea gas exchange parameterization using novel conservation and volatile tracers, *Glob. Biogeochem. Cycles*, *14*, 373–387.

Wanninkhof, R. (1992), Relationship between wind speed and gas exchange over the ocean, *J. Geophys. Res.*, *97*, 7373–7382.

Wanninkhof, R., W. E. Asher, D. T. Ho, C. Sweeney, and W. R. McGillis (2009), Advances in quantifying air-sea gas exchange and environmental forcing, *Annu. Rev. Mar. Sci.*, *1*, 213–244.

Wanninkhof, R. and W. R. McGillis (1999), A cubic relationship between gas transfer and wind speed., *Geophys. Res. Lett.*, *26*, 1889–1892.

Zappa, C. J., W. E. Asher, A. T. Jessup, J. Klinke, and S. R. Long (2004), Microbreaking and the enhancement of air-water transfer velocity, *J. Geophys. Res.*, *109*, C08S16.